

LA-UR-99- 484

Approved for public release;
distribution is unlimited.

Title: **PHYSICS-BASED DAMAGE PREDICTIONS FOR
SIMULATING TESTING AND EVALUATION (T&E)
EXPERIMENTS**

Author(s): Francis L. Addressio, T-3
Mark W. Schraad, T-3
Matthew W. Lewis, ESA-EA

Submitted to: *LDRD Final Report to DOE Office of Scientific and Technical
Information (OSTI)*

DISTRIBUTION OF THIS DOCUMENT IS UNLIMITED 

MASTER

Los Alamos

NATIONAL LABORATORY

Los Alamos National Laboratory, an affirmative action/equal opportunity employer, is operated by the University of California for the U.S. Department of Energy under contract W-7405-ENG-36. By acceptance of this article, the publisher recognizes that the U.S. Government retains a nonexclusive, royalty-free license to publish or reproduce the published form of this contribution, or to allow others to do so, for U.S. Government purposes. Los Alamos National Laboratory requests that the publisher identify this article as work performed under the auspices of the U.S. Department of Energy. Los Alamos National Laboratory strongly supports academic freedom and a researcher's right to publish; as an institution, however, the Laboratory does not endorse the viewpoint of a publication or guarantee its technical correctness.

DISCLAIMER

Portions of this document may be illegible in electronic image products. Images are produced from the best available original document.

Physics-Based Damage Predictions for Simulating Testing and Evaluation (T&E) Experiments

Francis L. Addressio* (T-3), Mark W. Schraad (T-3) and Matthew W. Lewis (ESA-EA)

Abstract

This is the final report of a two-year, Laboratory-Directed Research and Development (LDRD) project at the Los Alamos National Laboratory (LANL). This report addresses the need to develop computational techniques and physics-based material models for simulating damage to weapons systems resulting from ballistic threats. Modern weapons systems, such as fighter aircraft, are becoming more dependent upon composite materials to reduce weight, to increase strength and stiffness, and to resist adverse conditions resulting from high temperatures and corrosion. Unfortunately, damaged components can have severe and detrimental effects, as evidenced by statistics from Desert Storm indicating that 75% of aircraft losses were attributable to fuel system vulnerability with hydrodynamic ram being the primary kill mechanism. Therefore, this project addresses damage predictions for composite systems that are subjected to ballistic threats involving hydrodynamic ram. A computational technique for simulating fluid-solid interaction phenomena and physics-based material models have been developed for this purpose.

Background and Research Objectives

This project focuses on modeling and simulation of a specific, yet extremely complex, phenomenon associated with ballistic threat penetration of a fluid-filled containment system. The phenomenon is known as hydrodynamic ram (HRam), and is an ever present issue with military aircraft from the standpoint of vulnerability and survivability. Statistics obtained from Desert Storm indicate that 75% of all combat aircraft losses were a result of fuel system vulnerability with HRam being the primary kill mechanism.

Within the context of military aircraft applications, an HRam event typically involves the impact and penetration of a fluid-filled structure (e.g., an aircraft wing or fuel tank) by armor-piercing incendiary (API) or high-explosive incendiary (HEI) projectiles, as depicted in Figure 1. The term HRam refers to the high fluid pressures that arise in these situations from the propagation of shock waves originating from the initial impact

event, and more importantly, from the detonation and explosion of the HEI rounds within the containment system. A typical HRam event, however, also involves underlying physical phenomena that become exceedingly complex due to the transmission of the physical effects through the interaction of the projectile, the fluid, and the structure, as well as the abnormally excessive structural damage that results from this fluid-solid interaction.

A fundamental aspect of reducing the vulnerability of aircraft to ballistic threat involves the ability of designers and analysts to accurately model the complex fluid and solid mechanical behavior resulting from HRam events. The nonlinear coupling that develops between the fluid and the solid materials involved in the HRam problem, however, dictates that a detailed mathematical description of the physical processes involved will be inherently complex. Further complicating this description are effects related to the potential presence of airflow over the structure, as well as details concerning the solid material behavior associated with the high degrees of deformation induced in the thin shells and the composite materials typically found in aircraft structural components.

A successful modeling effort must include the computational capability for treating not only the multiple fields and material phases (e.g., the solids, liquids, and gases) that are present in these problems, but the complex interaction between these fields and phases as well. In addition, the solid material behavior, the accumulation of material damage, and the various modes of structural failure—characteristic of large strain and high strain-rate structural response—must be modeled properly. A physically based modeling effort (as opposed to *ad hoc* or purely empirical methods) is desirable, because the models will be valid outside of the range of direct experimental verification.

Currently, the cost of test and evaluation experiments to quantify the ability of wing structures to survive HRam events is costly. The development of computational tools for simulating the interaction of ballistic projectiles with aircraft wings and internal fuel tanks could be used to aid in the design of military aircraft. Computational simulations also would be useful for reducing the number of candidate designs for composite and other solid structures, and for interpreting the deformation mechanisms observed in both controlled experiments and integrated tests. Furthermore, the availability of robust computational models could reduce the cost of validation experiments, which are necessary for the design of engineering structures.

Importance to LANL's Science and Technology Base and National R&D Needs

This project is closely related to another LDRD project entitled “Hierarchical Simulation R&D Testbed for Test and Evaluation (T&E)”. The ultimate goal of this

related project is to develop a research and development (R&D) test bed for use in studying the representation of military forces—from the individual system (e.g., an aircraft), to the platoons or cohorts (e.g., few-on-few aircraft), up through four levels of echelon (e.g., to many-on-many aircraft). Integration of physics-based (i.e., continuum mechanics) models into the so-called “human-in-the-loop” war-fighting simulations, such as JointSim and SAMSON, will be undertaken such that the final product will be a next-generation simulation methodology for complete assessment of the phenomenological problem of battle damage occurring through the higher entities of war fighting. The fundamental pillar of the war-fighting modeling and simulation capabilities rests on the physics-based phenomenology, that is, on the computational robustness necessary to solve large-scale, complex physics problems. The information gained from the phenomenological assessment is used as input into the higher-level models. These combined projects address a fundamental need to support testing and evaluation of military systems through the use of modeling and simulation. Naturally, the specific problem of military force representation is a Department of Defense (DoD) concern. The overall idea of using modeling and simulation to support weapons systems design, however, is very closely related to the primary mission of LANL. Further information on the hierarchical modeling and simulation of war-fighting systems is available through LDRD/PD 97-535.

Additionally, the specific problem of HRam and how it relates to the vulnerability and the survivability of military aircraft also is primarily a DoD concern. The current physics-based modeling effort parallels other efforts by researchers within the DoD complex to develop a simulation capability for predicting the effects of HRam on military aircraft components. The problem of containment for hydrodynamic tests, however, plays a central role in the primary mission of LANL as well. Design of a low density containment vessel will provide a high-leverage step towards next-generation, high-resolution radiography with protons. Development of a simulation capability for shock wave propagation and interaction with a containment structure, and for the corresponding impact and penetration of the high-explosive casing fragments, would be the first step in this design process. Several sample calculations (see the section below on simulations) using the approach outlined below already have served as the inspiration for pursuing further experimental and computational efforts for Fiscal Year 1999.

Scientific Approach and Accomplishments

The approach taken to provide a predictive capability for modeling and simulation of HRam events involves two very different aspects. First, an appropriate computational

approach must be taken in order to develop a capability for solving fully coupled fluid-solid interaction problems. Second, robust, efficient, physics-based material models must be developed and incorporated into the computational technique to assure proper representation of the material behavior in a given HRam problem. These separate, but related, approaches are outlined below, followed by the results from several sample simulations. Several concluding remarks summarize the overall accomplishments of this research project.

1 Computational Approach

A unique approach to modeling fluid-solid interaction phenomena has been developed. This new approach involves the use of a library of continuum mechanics codes known collectively as CFDLIB. The library represents a collection of computational methods and modeling techniques, developed over several decades by scientists in the Theoretical Division's Fluid Dynamics Group, for modeling compressible flow involving single fluids. As the name implies, CFDLIB was originally intended for use in solving computational fluid dynamics (CFD) problems. Over the past decade, however, the library has subsequently been modified, extended, and generalized in an effort to provide solutions to a wider range of computational continuum mechanics problems.

1.1 Code Development and Capabilities

The first major modification made to the library of codes involved the addition of multifluid and multiphase capabilities (see [1] and [2]). In addition, a computational technique was employed that allowed for conservation of mass, momentum, and energy—for each material in a given problem—in the material's own Lagrangian or Eulerian frame of reference. This was the essential capability that allowed subsequent development of the immersed boundary method, which was the second major modification made to CFDLIB (see [3] and [4]). In this method, the dynamics of a solid body immersed in a fluid field are represented through the use of Lagrangian markers. The state of the immersed solid is evolved in time as it is influenced by the dynamics of the surrounding fluid. In this way, the fully coupled nature of the fluid-solid interaction problem is always preserved. A particle method was included in the library for the time-explicit evolution of the deviatoric stress in the immersed Lagrangian solid. The dynamic response of the immersed solid body could then be computed with arbitrary material response laws that include a variety of plasticity and material failure models.

Currently, all of the codes in the library are related to one another by virtue of a set of common features. These features include the use of a finite-volume computational scheme, in which all state variables are cell-centered; an arbitrary Lagrangian-Eulerian (ALE) split computational cycle for solving the governing equations of motion; a particle-in-cell (PIC) method that is used for solid material modeling; and a multiblock data structure that enables highly efficient processing on modern supercomputers.

The ALE technique allows one to choose—on a material-by-material basis—either the Lagrangian or Eulerian frame of reference for satisfying the conservation laws. This capability is essential for the fluid-solid interaction problem. In general, the motion of a liquid or gas would be computed in an Eulerian frame, while a Lagrangian frame would be used to compute the motion of a solid. The dynamic behavior of a solid material may depend strongly on the history of the straining motion. Accuracy of the solid dynamic calculations depends on the accuracy of the computed strain history, as well as on the accuracy of the present state of stress. Calculations in a Lagrangian frame of reference provide the best possible representation of the history variables and allow for arbitrarily large deformations of the material. For a Newtonian fluid, however, the dynamic behavior typically depends only on the current state of the material and not on variables describing the history of the straining motion. In this case, use of the Eulerian frame of reference is more natural, and in certain cases, the Eulerian frame can be the most practical frame on which to carry out the dynamic simulations.

The marriage of the particle method with the original ALE technique was accomplished following the procedure outlined in [5]. The PIC method described in [6] was included to allow for solid material modeling (see also [7], [8], [9], and [10]). Modeling the behavior and failure of solid materials is greatly simplified with this new particle technique. Although there is an underlying computational grid on which the numerical calculations are performed, one never has to explicitly define a mesh connectivity for the solid material. Therefore, the method provides a Lagrangian description of the solid mechanical behavior without the usual numerical complexities of mesh tangling and free-surface creation associated with classical Lagrangian finite-element solutions. In this sense, this new technique has strong advantages over the majority of ALE codes and purely particle-based techniques.

Elasto-plastic and visco-plastic constitutive models, which describe the large strain and high strain-rate dynamic behavior of metals and polymers, have been incorporated into the previously mentioned PIC method. A micromechanics-based constitutive model that describes the macroscopic behavior of fiber-reinforced and layered composite materials has also been included. Furthermore, material failure models have

been implemented for homogeneous materials and for the homogeneous constituents in heterogeneous materials. And finally, debonding and delamination models have been included for describing the interfacial and interlaminar behavior of composite materials.

Arbitrary equations of state have been included for determining the temperature- and specific-volume-dependent pressure for the various materials involved in a given problem. All flow speed regimes—ranging from fully incompressible to hypersonic—are accessible in the library. Multifield and multiphase computations have been enabled allowing an arbitrary number of material classes. Furthermore, one can choose to represent the coexistence of both compressible and incompressible materials in the same simulation. Each material class in a given problem has its own set of conservation equations, and therefore, its own set of state variables (e.g., velocity field, strain rate, etc.). The fully coupled nature of the fluid-solid interaction problem is accounted for through mass, momentum and energy exchange terms that are derived and included in the exact form of the conservation equations.

Analyses involving geometries of arbitrary complexity can be treated with either structured or unstructured mesh capabilities. And finally, the design of each computational code in the library is modular, making the development of programs for specialized applications exceptionally fast.

Each computational code contained in CFDLIB has been developed and tested in both two- and three-dimensions and is capable of solving a wide range of continuum mechanics problems. Therefore, at this stage in the code development, the scheme is fully general and has been shown to be practical for a broad class of fluid-solid interaction problems. The codes have been developed with the “sophisticated” user in mind. The experienced computationalist can set up and solve a large variety of problems quickly, with little instruction from manuals and internal documentation. Hence, CFDLIB is a tool most useful to the researcher interested in exploring highly specialized problems in continuum mechanics.

This library of computer codes has been designed to serve as a research tool for the investigation of problems in complex material dynamics. The code development already has served to spawn the creation of some very specialized numerical analysis methods. The immersed boundary capability that has been enabled thus far in CFDLIB has all of the properties that are desirable for fluid-solid interaction problems with arbitrarily large deformations of the solid—up to and including material failure. Therefore, as a vehicle for exploration of such problems, the computational technique offered by CFDLIB is ready to be exercised. Potential fluid-solid interaction applications include wind and wave action on buildings and bridges, blast loading of complex

structures, material casting and forming processes, interaction between submerged structures and bubbles, earth penetration, propagation of blast waves in porous media, fluidized-bed motion, and most importantly, HRam.

1.2 Theoretical Basis

The numerical method developed for use in solving multifluid flow problems is an extension and generalization of the so-called semi-implicit procedure known as the implicit continuous-fluid Eulerian (ICE) method for single-fluid flow (see [11] and [12]). This method involves a computational scheme that is stable for any value of the Courant number based on the sound speed. In the incompressible limit, the ICE method becomes essentially identical to the Marker and Cell (MAC) method. The two schemes, therefore, are closely related, and as a result, problems involving equations of state or those exhibiting constant material densities can be addressed with the same computational code. The ICE method has been extended to a nonstaggered mesh framework, in which all state variables are cell-centered. The method has also been generalized to treat problems involving multiple material fields with separate sets of conservation laws. The term semi-implicit is used here in the sense that the implicitness is limited to the Lagrangian part of the equation system (i.e., the pressure iteration). The purpose for the semi-implicit capability is to remove any stability conditions on the time-step due to the propagation of pressure waves.

This computational technique also belongs to the larger class of numerical procedures known as finite-volume methods. In these methods, the integral form of each conservation law is discretized on an underlying mesh of arbitrary volumes. Naturally, the computational scheme is intended for time-dependent equations. If a steady state is of interest, however, it is found simply by incrementing through time until the state variables cease to change from time step to time step.

To solve the governing equations of motion for a given continuum mechanics problem, the finite-volume formulation has been combined with an ALE split computational cycle. The ALE technique itself is not unique to these types of problems, however, this new computational approach involves the combination of multifield ALE techniques and PIC methods. The PIC method is included for characterizing the stress-strain response of the solid materials involved in a given calculation and for evolving the stress state in these materials through the use of appropriate constitutive models. The PIC method is particularly suited to applications involving fluid-solid interaction, since the method provides a Lagrangian description of the solid material behavior. Inaccuracies that arise from issues associated with advection in an Eulerian description, therefore, are

avoided. Furthermore, the technique provides solutions for high degrees of deformation in the solid materials, follows deformation through initial material failure, and models problems involving penetration and perforation without the numerical problems typically associated with classical Lagrangian solutions.

In this way, a mixed-frame method for solving fluid-solid interaction problems has been developed. This new computational technique involves five primary steps for advancing the state of the materials using this mixed-frame approach:

Step 1. The current time-dependent variables are interpolated into a common frame of reference—the Eulerian frame, which is furnished by an underlying computational grid. This step may be thought of as an “initialization” of the state of the materials on the grid.

Step 2. The acceleration due to a solid material stress is computed in the Lagrangian frame and interpolated onto the grid. At this point, the stress in the Lagrangian solid is also updated together with any history variables that require updating.

Step 3. The dynamics due to the “physics” of the fluid acceleration, the work, the dissipation, the heat conduction, the mass exchange, the momentum exchange, etc. is computed on the grid (i.e., in the Eulerian frame).

Step 4. The change in state is interpolated from the grid back to the Lagrangian frame for those materials conserved in that frame of reference. This includes updating marker locations using the interpolated grid velocities (this procedure is the hallmark of the FLIP technique).

Step 5. The state is advected for those materials conserved in the Eulerian frame.

Collectively, these five steps offer a new computational approach to fluid-solid interaction modeling.

2 Material Model Development

As previously mentioned, the PIC technique uses suitable constitutive representations for describing the mechanical response of the solid materials involved in a given continuum mechanics calculation. Nonlinear, inelastic, anisotropic material

response models, which include effects due to work hardening, thermal softening, strain-rate dependence, and material failure, have been incorporated into the PIC methodology. Plasticity models, which accurately account for the hardening phenomena due to strain and strain-rate effects, have been developed for describing the elasto-plastic behavior of metals. Constitutive models have also been constructed for characterizing the rate-dependent, visco-plastic deformation of polymers. Models for various modes of structural and material failure have been incorporated into the constitutive models. And finally, efforts have been made to mitigate the usual numerical complexities that develop with the incorporation of failure phenomena into continuum mechanics analyses.

Modern weapons systems are becoming increasingly dependent on composite materials for increased structural strength and decreased weight. For these more complex material systems, the overall or macroscopic mechanical response is strongly dependent on the response of the individual constituents and material interfaces one finds within the material system. The mechanical response at this smaller structural level is typically referred to as the microscopic or microstructural mechanical response. Descriptions of the macromechanical behavior and the corresponding damage (e.g., debonding and delamination) in composite materials are obtained by employing a micromechanics-based homogenization technique known as the Method of Cells (MoC). For details concerning this homogenization technique see [13]–[19]. In this technique, details concerning the micromechanical behavior of the individual constituents and their interfaces are used to develop macromechanical response laws for the overall composite material behavior. Damage and failure models for the individual constituents, as well as debonding and delamination models, are included in the homogenization technique. The method is general and provides constitutive models for fiber-reinforced, particle-reinforced, and layered composites; fabric and woven composites; as well as functionally graded materials.

Under large strain and high strain-rate loading conditions, advanced structural composites can experience both large volumetric and shear stress states. Accurate numerical simulations for the mechanical response of these anisotropic materials under high strain-rate conditions must include the effects of nonlinear elasticity, as well as inelastic phenomena such as plasticity and damage. Modeling composite materials involves the additional complexity of requiring constitutive models for the interfaces as well as the individual constituent materials. Interfacial debonding between the fiber and matrix materials and delamination between the layers of a laminated composite provide two important failure mechanisms within composite structures. Physically based

material models (as opposed to *ad hoc* or empirically based models) are desirable for characterizing the thermomechanical response of composite materials.

Computational expediency, however, requires material models that are numerically robust and computationally efficient. As shown in Figure 2, the length scales necessary to model the detailed response of the individual constituents and the material interfaces within a composite material are much smaller than the length scales of typical engineering structures. Consequently, attempting to numerically resolve the composite microstructure is impractical at best. By employing a macromechanical approach, however, the composite material may be modeled as an equivalent, homogeneous, anisotropic material. Using this type of approach, details concerning the material microstructure are necessarily ignored. As a result, the macromechanical description is convenient and may be implemented easily into computational continuum mechanics analyses. Unfortunately, classic mechanics principles such as plastic incompressibility, yield surface convexity, and normality of the plastic strain-rate, which may apply to the individual constituents, may not be valid for the composite material itself. Therefore, macromechanical descriptions of composite material behavior are often dependent on the existence of a large experimental database for calibrating the material models.

Conversely, a micromechanical approach may be used to model the composite material as well. In this type of an approach, a homogenization technique, which seeks to describe the volume averaged stress response of the material under consideration, is used to develop appropriate macroscopic constitutive relations. Naturally, details concerning the micromechanical response of the individual constituents and the interfaces within the composite material are included in the analysis. The microstructure of the composite is idealized by a periodic representative volume element (RVE), as shown in Figure 3. The macromechanical response of the material is then obtained as an appropriate average of the responses of the individual constituents and interfaces over the entire RVE. This type of approach, therefore, eliminates the need to provide a detailed description of the material response at the material's microstructural level. Furthermore, the homogenization technique has been extended to include phenomena inherent to the large strain and high strain-rate loading conditions characteristic of ballistic impact events.

2.1 The Method of Cells

The Method of Cells is a homogenization technique that has demonstrated tremendous versatility. The method is applicable to general loading conditions, it is compatible with a wide variety of constitutive relations for the individual constituents and the interfaces within a composite material, and it is easy to implement as the material

model in existing continuum mechanics analyses. The Method of Cells has been employed for the purposes of calculating the thermomechanical response of a variety of engineered composites with very good success. The method is applicable to any ordered composite that can be idealized with a microstructural RVE that generates the entire composite material through spatially periodic repetition. It is assumed that the characteristic microstructural length is very small relative to the overall structural dimensions of the composite. In this sense, the entire RVE maps into a point in the continuum coordinate system (see Figure 3). The macroscopic stress state calculated for the RVE is taken to be the stress-state at the corresponding location in the equivalent, homogeneous continuum. With a knowledge of the response of the individual constituent materials, the homogenized stress state is then obtained as the solution for the mechanical response of the RVE to an applied macroscopic strain.

2.1.1 Micromechanical Model

A detailed development of MoC is provided in the literature, and will, therefore, not be included here. In general, the development proceeds in four steps:

Step 1. An idealized RVE is identified.

Step 2. Strains and material models are defined on the micromechanical level.

Step 3. Continuity of displacements and tractions across material interfaces are imposed in an average sense.

Step 4. Suitable averages are provided for the micromechanical stresses resulting in the macromechanical response of the RVE.

In this method, a typical RVE will be comprised of a number of different subcells (hence the name Method of Cells). In general, each subcell will be associated with one of the constituent materials within the composite. Constitutive models are, therefore, specified for each of the constituent materials. The model provides only a quasi-static response for the RVE, however, the solution to the continuum conservation equations provides the transient response of the composite structure. This is sufficient for applications with spatial resolutions that are much larger than the microstructural dimensions of the material and with time scales that are longer than the wave transit times through the RVE. Since

the microstructural dimensions are typically very small, many structural and solid mechanics applications meet these restrictions.

2.1.2 Constituent Models and Interfacial Behavior

Once the material response laws for the individual constituents and the interfaces within the composite material have been defined, the response of an equivalent homogeneous continuum may be obtained by averaging over the response provided by the micromechanical models. As previously noted, one of the primary advantages offered by this micromechanical approach is that the material response is defined for each of the constituents within the composite material rather than for the overall composite itself. Inelastic deformation of the individual constituent materials, typically associated with plasticity and damage, is included in the formulation. The nonlinear elastic deformation of the constituent materials, which is necessary for capturing high strain-rate phenomena, is also treated. Failure models are incorporated in the material descriptions and are dependent on the micromechanical stress-state in the material. A simple interfacial decohesion model provides for damage to the fiber-matrix interface. And finally, an approach for modeling layers of fiber-reinforced laminae is included with an interlaminar decohesion model that provides a means for investigating delamination phenomena.

2.1.3 Numerical Implementation

As presented in the previous sections, MoC is suitable for implementation in a continuum mechanics analysis. Typically, for solutions to large deformation, high strain-rate problems, time-explicit numerical techniques are employed. For each time cycle in a given problem, the continuum state is obtained from solutions to the conservation equations for mass, momentum, and energy, as well as from constitutive models for the stress-strain response of the materials under consideration. Solutions to the macromechanical conservation equations provide the material constitutive models with the macromechanical velocity gradients or rates of deformation, as well as the internal energy. This information is used to update the stress-states in the individual constituent materials. Both the micromechanical and macromechanical stress-states, which are consistent with the macromechanical strain state, are obtained from the solution to the homogenization technique. The macromechanical stress-state is then returned to the continuum analysis, and the solution for another time cycle is pursued.

For large-scale, continuum-mechanics simulations, providing a detailed resolution of the composite microstructure is impractical. Furthermore, only the macroscopic response of the composite material is required for the continuum analysis. A solution

technique that can be conveniently implemented in a continuum analysis is provided by MoC. The robustness of this approach is dependent on the constitutive representation used to describe the material response of the individual constituents and the interfaces within the composite material. Therefore, the computational cost of using this technique is dependent on the details of the problem that require this level of modeling.

2.2 Classic Plate and Shell Theory

One of the main difficulties in simulating the dynamic behavior involved in an HRam problem arises because the walls of fluid containment systems are usually very thin relative to the corresponding overall structural dimensions. Typical wall thicknesses may be measured in millimeters while the fuel tank or aircraft wing dimensions may be measured in meters. A computational grid that resolves both length scales would be awkward, to say the least.

This problem is alleviated by treating thin structural components with classic plate theory. Hence, the thickness of a thin wall is not resolved, except in an integral sense, so the grid spacing can be selected on the basis of the overall structural dimensions alone. The plate model is “overlaid” on top of the model for homogeneous materials. The multiple stress layers, the plate normal for each mass point, and the corresponding rate of rotation are the only essential extensions that are required. In exchange for this added bit of complexity, the need to resolve dynamics through the thickness of the plate is removed. The center-of-mass velocity, plus the normal and rotation rate furnish a complete velocity representation. A layer-wise gradient is used to form the local rate of strain that is needed to update the stress in each layer using the same material response model that is already in place for homogeneous materials. For a more detailed account of how this theory has been incorporated into the overall modeling effort see [20].

2.3 Improved Shell Formulation for Composite Materials

Thin, laminated, composite structures have many potential engineering applications—including use as aircraft wing and fuselage skins. Laminated structures, however, are susceptible to failure by delamination between layers, due to the low transverse strength at the interlaminar interfaces. Delamination results in significant degradation of the mechanical response characteristics of these structural components. Therefore, before all of the potential applications of laminated composites can be realized, analytical tools that can accurately predict the behavior of delaminated structures must be developed. A generalized, higher-order theory for modeling the delamination behavior of thin composite plates and shells has been developed (see [21] and [22]). A higher-order

theory is necessary for efficient modeling of HRam phenomena, since these problems typically require the simulation of geometries that are large relative to the thickness of the aircraft wing skin (as discussed above). The theory is also required for accurately modeling the stress distribution through the thickness of the thin plates and shells—information that is ultimately required for accurate delamination prediction.

3 Simulations

The following series of figures depict select results obtained using the CFDLIB family of continuum mechanics codes to perform two-dimensional, axisymmetric simulations involving the impact and penetration of a 23-mm steel projectile into a graphite/epoxy composite fuel tank. These numerical results serve, in part, to demonstrate the HRam modeling and simulation capabilities currently offered by CFDLIB, the corresponding unique computational technique, and the library of constitutive models that have been developed for describing large strain and high strain-rate deformations of both homogeneous and heterogeneous solid materials.

In Figure 4, the reference (i.e., the undeformed) configuration of the cylindrical fuel tank is shown at the time of initial projectile impact. At the time of impact, the projectile is traveling with a velocity of 60.96 cm/ms (609.6 m/s). The 4340 steel projectile is a solid, right-circular cylinder (red) and is modeled using a rate-dependent, isotropic, elasto-plastic constitutive model. For simplicity, the contained fluid is water as opposed to fuel. Nevertheless, both the water (blue) and the surrounding air (black) are modeled as compressible fluids using a Mie-Gruneisen equation-of-state. Both the entrance and the exit plates, as well as the walls of the cylindrical fuel tank (green), are composed of a unidirectional, graphite/epoxy (IM7/8551) composite material with total plate and wall thicknesses of 0.678 cm. These thicknesses are equivalent to those of layered composites comprised of 64 individual laminae. The composite material is modeled using the Method-of-Cells homogenization technique, in which each of the individual constituents (i.e., the fiber or the matrix material, respectively) is modeled using either an anisotropic or an isotropic, visco-plastic constitutive model. Furthermore, within this constitutive model, the effects of both fiber-matrix debonding and matrix cracking are considered as a means for allowing structural failure of the composite material.

The fuel tank configuration at the time of initial projectile impact is shown once again in Figure 5, along with the corresponding deformed configurations of the tank at several times after impact. At time $t = 0.090$ ms, the steel projectile already has penetrated into the target plate, failure of the plate resulting from debonding of the fiber and matrix materials has commenced, and complete perforation of the target plate has

ensued. At time $t = 0.210$ ms, the target plate has failed completely, allowing the projectile to penetrate deeper into the fuel tank with the residual velocity that remains after the impact and penetration event. At this point, the projectile is pushing a composite plug through the water as it travels further into the cylindrical fuel tank. Here, further impedance to the motion of the projectile is provided only by viscous drag. Finally, at time $t = 0.300$ ms, the steel projectile has reached a penetration depth that is equivalent to the point of HE detonation in a corresponding 23-mm HEI round. The results presented in this figure illustrate several important characteristics of the high-rate deformation and subsequent failure of the target plate that must be captured in this type of simulation. First, notice the relatively small hole that has been generated in the target plate. A small-radius hole is expected since the rates of deformation are high, and therefore, the resulting failure of the composite material is brittle in nature. Second, notice the increasing outward (i.e., the upward) displacement of the target plate as the projectile penetrates deeper into the cylindrical fuel tank. Again, this is expected, since the contained water will behave as a nearly incompressible fluid. This phenomenon further illustrates the ability of this computational technique to capture the fully coupled nature of the fluid-solid interaction problem.

The deformed configuration of the cylindrical fuel tank at the time of HE detonation is shown once again in Figure 6. Here, the size of the figure has been enhanced to better illustrate some important features of the deformation and failure of the target plate, and the corresponding fluid-solid interaction in the region near the initial impact zone. First, notice the relatively minor deformation of the solid steel projectile as compared with the larger deformations and complete failure of the composite plate. This difference in behavior is expected, since the steel projectile is solid and has tremendous momentum as it impacts the relatively thin composite plate. In addition, aside from the onset of plasticity, no other failure model was included in the constitutive description of the steel. If the projectile had been modeled as an actual HEI round (i.e., an HE material surrounded by a steel casing that may fail), then the deformation of the projectile (and most likely, the deformation of the target plate) would have been significantly different. Second, careful inspection of the target plate also shows localized deformation (i.e., necking) in the composite material at the locations where fracture has occurred. This type of solid material behavior often causes significant numerical problems in classical, Lagrangian, finite-element solutions. A final point of interest with regard to the fluid behavior is noted in the cavitation that is produced by the motion of the projectile and the composite plug through the water. Here again, the capability of capturing the fully coupled nature of the fluid-solid interaction is demonstrated.

Finally, in Figure 7, the density of the water is shown at the time of initial projectile impact and several later times to show the propagation of the weak pressure wave that results from the initial impact event. Naturally, at the time of initial projectile impact the density of the water is uniform. At time $t = 0.090$ ms, the steel projectile has perforated the target plate and displaced the water, while a weak pressure wave resulting from the impact event has propagated through the thin composite plate, and subsequently, into the contained water. As expected, the pressure wave is spherical in shape and propagates through each medium at the corresponding speed of sound. At time $t = 0.210$ ms, the target plate has completely failed and the projectile has penetrated deeper into the tank. At this time, the pressure wave has propagated further and cavitation zones have developed on either side of the projectile path. At time $t = 0.300$ ms, the steel projectile has reached the depth corresponding to HE detonation. At this time the pressure wave has been reflected off of the tank walls and the cavitation zones have become much more pronounced. It should be noted that if an HEI round were to detonate at this point in time, then the resulting pressure wave would be much stronger than the weak pressure wave that results from the impact event. Naturally, this stronger wave would have more devastating effects on the deformation of the entrance and exit plates and the remainder of the cylindrical tank. Nevertheless, the computational technique and the solid material models that have been employed in the present simulation are certainly capable of capturing these effects.

To illustrate the high-explosive modeling capabilities offered by CFDLIB a variant of the same experiment involving high-explosive detonation was also pursued. The focus of this simulation was the detonation phase of the high explosive and the subsequent pressure wave development in the contained fluid. Therefore, to facilitate the calculation, the tank wall was modeled as aluminum using an elasto-plastic constitutive model with a failure strain of 0.262. The projectile was modeled as steel, again with an elasto-plastic constitutive law, however, no failure strain was specified for this material. The geometry of the projectile was meshed in detail, allowing for representation of the taper of the projectile tip and of the cavity for the high explosive.

At the time this simulation was carried out, CFDLIB was limited to simulating the behavior of four material phases per calculation. This limitation, however, is currently being remedied for simulations involving many Lagrangian phases. Nonetheless, in this simulation, it was necessary to use the same material phase for both the high explosive material and the surrounding air. To do this, the initial density of the air (an Eulerian phase in this calculation) was increased to the appropriate density inside the projectile. Additionally, to ensure pressure equilibrium, the temperature of this phase in this region

was set to an arbitrary low value. The BKW equation of state for the high explosive products was then used to simulate the high-explosive detonation (for further examples of this type of simulation see [23]).

At a time of 200 ms, the explosive products in the projectile were given a higher temperature (2718 K) to represent the complete burn of the high explosive. Unfortunately, by this time the explosive products have already begun to “leak” from the projectile due to Eulerian diffusion. This numerical phenomenon was not preventable—even with a higher-order advection scheme. A solution to this nonphysical phenomenon involves the use of a Lagrangian phase for the explosive products and an Eulerian phase for the air surrounding the projectile and the tank. As previously mentioned, a data structure that will allow the inclusion of a single Lagrangian velocity field that represents different materials is being implemented. Plots of the Lagrangian marker positions and the corresponding pressure field at 220 ms after initial projectile impact (i.e., at 20 ms after high-explosive detonation) are shown in Figure 8 and Figure 9, respectively. The resulting pressure wave is much stronger than the pressure wave that results from the initial impact event alone.

Finally, with the previously mentioned issues of containment for hydrodynamic tests in mind, the modeling capabilities offered by the computational technique within the CFDLIB family of continuum mechanics codes were used to simulate the shock-wave loading, as well the subsequent impact and penetration by high-explosive casing fragments, of a spherical composite containment vessel. The initial problem set-up is illustrated in Figure 10a. Here, a specified mass of high explosive (red) is surrounded by a thin steel casing (green). The explosive is placed at the center of a spherical containment vessel (blue). The vessel is a thin shell of Spectra composite. After detonation of the high explosive, a shock wave propagates through the contained fluid medium, followed by the steel casing fragments, as shown in Figure 10b. With these dynamics in mind, two different simulations were used to study the effects on the containment vessel. The problems of shock wave loading and fragment impact and penetration were decoupled and studied separately, as shown in Figures 10c and 10d.

In the first simulation a temperature “hot spot” was placed at the center of the containment vessel as a means of representing the energy of the explosion without having to simulate the full detonation event. The thin composite shell of the vessel was modeled as an equivalent homogeneous solid with the macroscopic properties exhibited by the Spectra composite material. After the initial explosion event a shock wave propagates through the air contained within the vessel, as shown in Figure 11a. When the shock front reaches the thin composite shell, it reflects off of the container and a pressure wave

continues to propagate through the solid walls. Due to the thickness of the containment vessel walls, however, the deformations remain very small and the levels of stress and strain do not approach values that threaten failure of the material.

In the second simulation, a square, tantalum projectile impacts a thin flat plate of Spectra composite with a velocity of 2000 m/s. An isotropic, elasto-plastic constitutive model was again used to represent the equivalent homogeneous solid material properties, and a two-dimensional, plane-strain solution was pursued. Figure 12 depicts the penetration event at 25, 60, and 100 ms after initial impact (Figures 12a, 12b, and 12c, respectively). These figures show the value of the second invariant of the stress deviation tensor. The results show the development of a shock wave resulting from the impact event and the propagation of this shock wave through the solid material. The results also show the impact crater as it develops (the projectile particles have been removed for clarity). At approximately 100 ms the projectile comes to rest, indicating that for a projectile of that mass and velocity, the container walls are sufficiently thick to prevent perforation. Notice, however, that the entire plate has deformed under the conditions of the impact event.

4 Conclusions

As the previous simulations show, CFDLIB—in its present stage of development—is capable of solving fully coupled, fluid-solid interaction problems. Furthermore, the computational technique and material models currently being used offer a unique and useful modeling procedure for exploring problems involving hydrodynamic ram. Alleviation of several modest code limitations and inclusion of additional material models would result in an immeasurably valuable research tool.

References

- [1] Kashiwa, B. A. and Rauen Zahn, R. M., "A Multimaterial Formalism" Numerical Methods in Multiphase Flows 1994, **185**, 149–157, (1994).
- [2] Kashiwa, B. A., Padial, N. T., Rauen Zahn, R. M. and VanderHeyden, W. B., "A Cell-Centered ICE Method for Multiphase Flow Simulations," Numerical Methods in Multiphase Flows 1994, **185**, 159–167, (1994).
- [3] Kashiwa, B. A., Lewis, M. W. and Wilson, T. L., "Fluid-Structure Interaction Modeling," Los Alamos National Laboratory Report LA-13111-PR, Los Alamos, New Mexico, (1996).
- [4] Kashiwa, B. A. and Lewis, M. W., "Fluid-Structure Interaction Modeling," Los Alamos National Laboratory Report LA-13255-PR, Los Alamos, New Mexico, (1997).
- [5] Brackbill, J. U. and Ruppel, H. M., "FLIP: A Method for Adaptively Zoned, Particle-in-Cell Calculations of Fluid Flows in Two Dimensions," Journal of Computational Physics, **65**, 314–343, (1986).
- [6] Sulsky, D., Chen, Z. and Schreyer, H. L., "A Particle Method for History-Dependent Materials," Computer Methods in Applied Mechanics and Engineering, **118**, 179–196, (1994).
- [7] Brackbill, J. U., Kothe, D. B. and Ruppel, H. M., "FLIP: A Low-Dissipation, Particle-in-Cell Method for Fluid Flow," Computer Physics Communications, **48**, 25–38, (1988).
- [8] Sulsky, D. and Brackbill, J. U., "A Numerical Method for Suspension Flow," Journal of Computational Physics, **96**, 339–368, (1991).
- [9] Sulsky, D., Chen, Z. and Schreyer, H. L., "The Application of a Material-Spatial Numerical Method to Penetration," Sandia National Laboratories Technical Report SAND91-7095, Albuquerque, New Mexico, (1991).
- [10] Sulsky, D., Zhou, S. and Schreyer, H. L., "Application of a Particle-in-Cell Method to Solid Mechanics," Computer Physics Communications, **87**, 236–252, (1995).
- [11] Harlow, F. H. and Amsden, A. A., "Numerical Calculations of Almost Incompressible Flow, Journal of Computational Physics, **3**, 80–93, (1968).

- [12] Harlow, F. H. and Amsden, A. A., "A Numerical Fluid Dynamics Calculation Method for All Flow Speeds," *Journal of Computational Physics*, **8**, 197–213, (1971).
- [13] Aboudi, J., "A Continuum Theory for Fiber-Reinforced Elastic-Viscoplastic Composites," *International Journal of Engineering Science*, **20**, 605–621, (1982).
- [14] Aboudi, J., "Effective Behavior of Inelastic Fiber-Reinforced Composites," *International Journal of Engineering Science*, **22**, 439–449, (1984).
- [15] Aboudi, J., "The Effective Thermomechanical Behavior of Inelastic Fiber-Reinforced Materials," *International Journal of Engineering Science*, **23**, 773–787, (1985).
- [16] Aboudi, J., *Mechanics of Composite Materials—A Unified Micromechanical Approach*, Elsevier, Amsterdam, (1991).
- [17] Aboudi, J., "Micromechanical Analysis of Thermo-Inelastic Multiphase Short-Fiber Composites," *Composites Engineering*, **5**, 839–850, (1995).
- [18] Paley, M. and Aboudi, J., "Micromechanical Analysis of Composites by the Generalized Cells Model," *Mechanics of Materials*, **14**, 127–139, (1992).
- [19] Addressio, F. L. and Aidun, J. B., "Analysis of Shock-Induced Damage in Fiber-Reinforced Composites," *High-Pressure Shock Compression of Solids*, **3**, (1995).
- [20] Lewis, M. W., Kashiwa, B. A. and Rauenzahn, R. M., "Fluid-Structure Interaction Modeling," Los Alamos National Laboratory Report LA-13415-PR, Los Alamos, New Mexico, (1998).
- [21] Williams, T. O. and Addressio, F. L., "A General Theory for Laminated Plates with Delaminations," *International Journal of Solids and Structures*, **34**, 2003–2024, (1997).
- [22] Williams, T. O. and Addressio, F. L., "A Dynamic Model for Laminated Plates with Delaminations," *International Journal of Solids and Structures*, **35**, 83–106, (1997).
- [23] Lewis, M. W. and Wilson, T. L., "Response of a Water-Filled Spherical Vessel to an Internal Explosion," Los Alamos National Laboratory Report LA-13240-MS, Los Alamos, New Mexico, (1996).

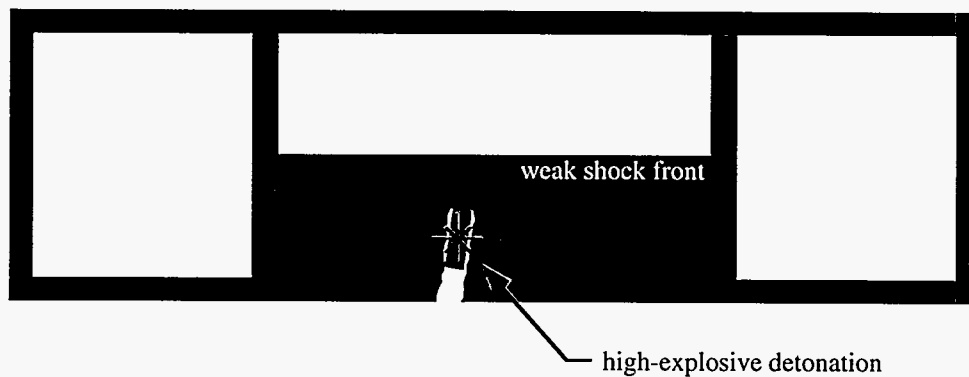
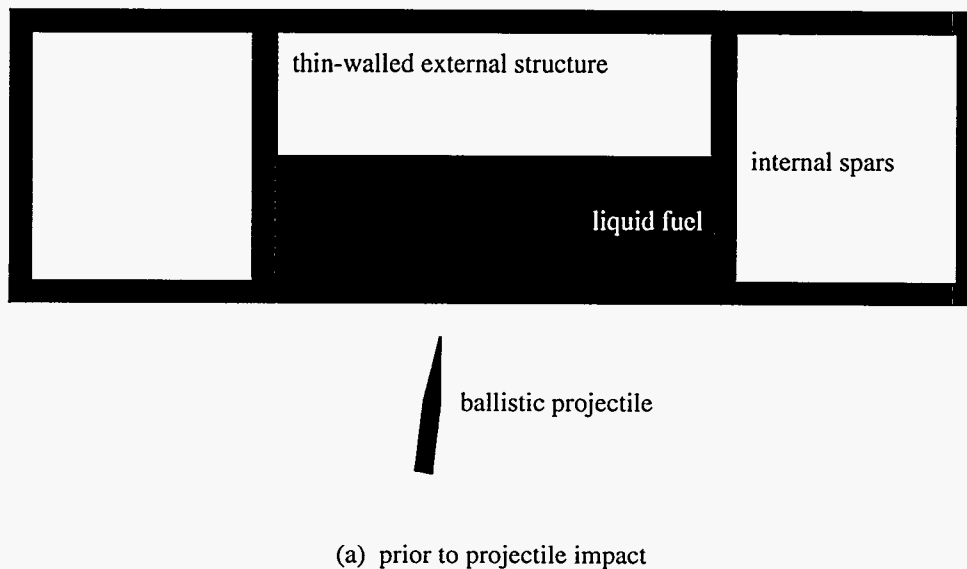


Figure 1: A typical HRam event involving the impact and penetration of an HEI projectile into a partially filled aircraft wing-tank. The projectile perforates the external composite structure and penetrates into the contained fuel where it detonates and explodes at a predetermined depth of penetration. The resulting damage will be greater than if the system contained no liquid due to the high fluid pressures that develop. This is the characteristic feature of the HRam problem.

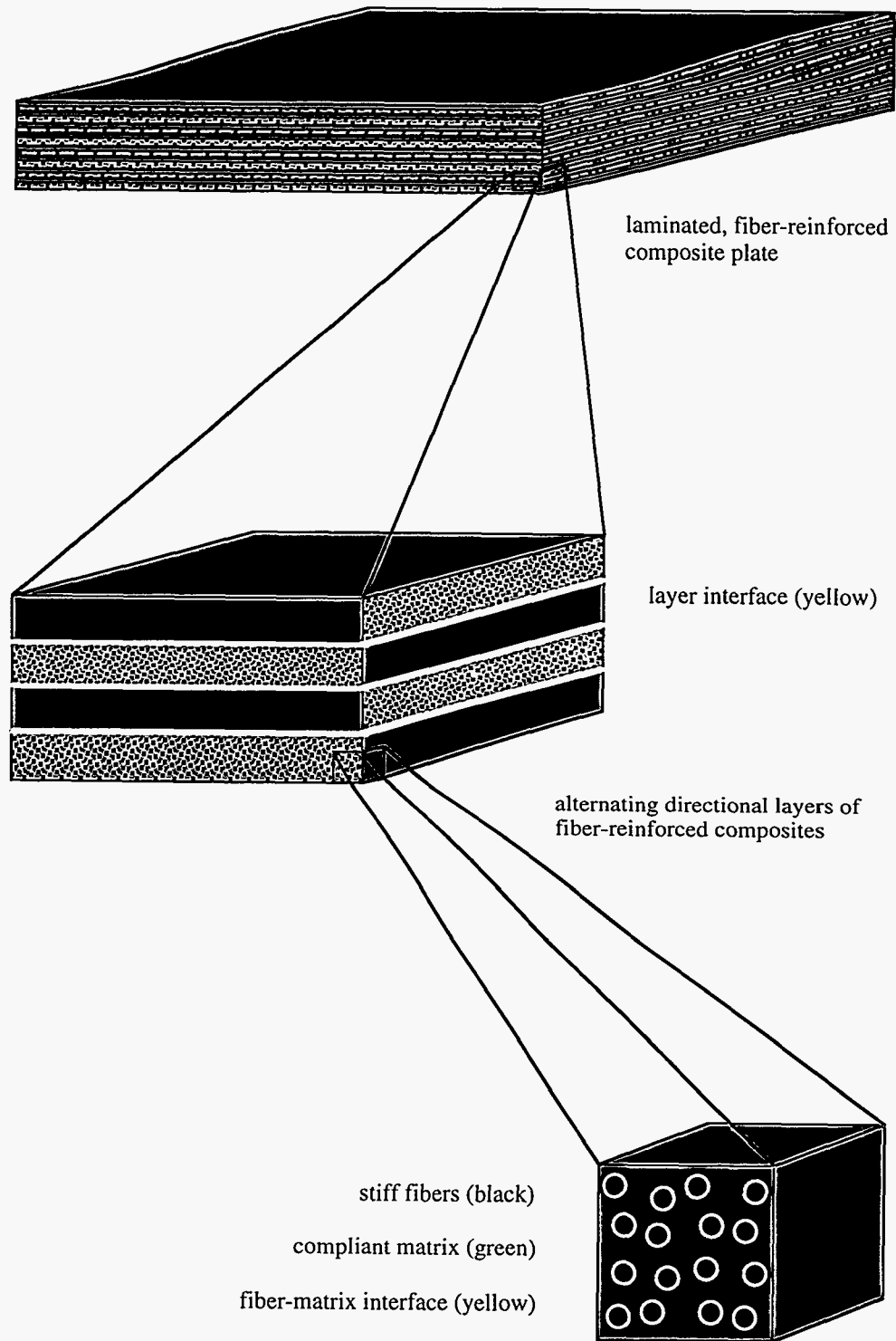


Figure 2: The various microstructural length scales found in a typical fiber-reinforced composite laminate. Note that the length scale corresponding to the fiber dimensions is much smaller than the overall structural dimensions of the composite plate.

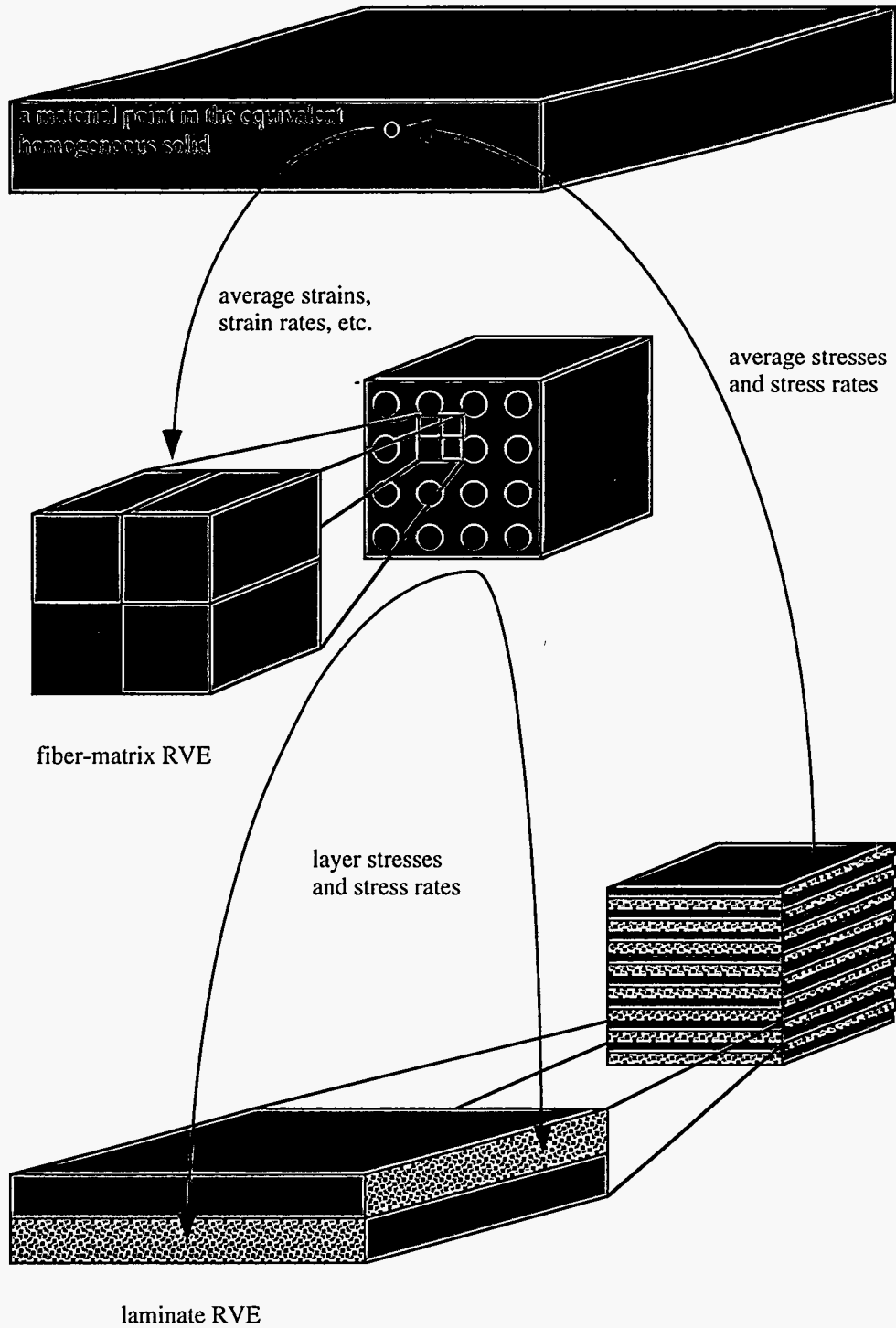


Figure 3: The Method of Cells (MoC) homogenization technique applied to a fiber-reinforced composite laminate. The microstructure of the composite material is idealized by a periodic representative volume element (RVE).

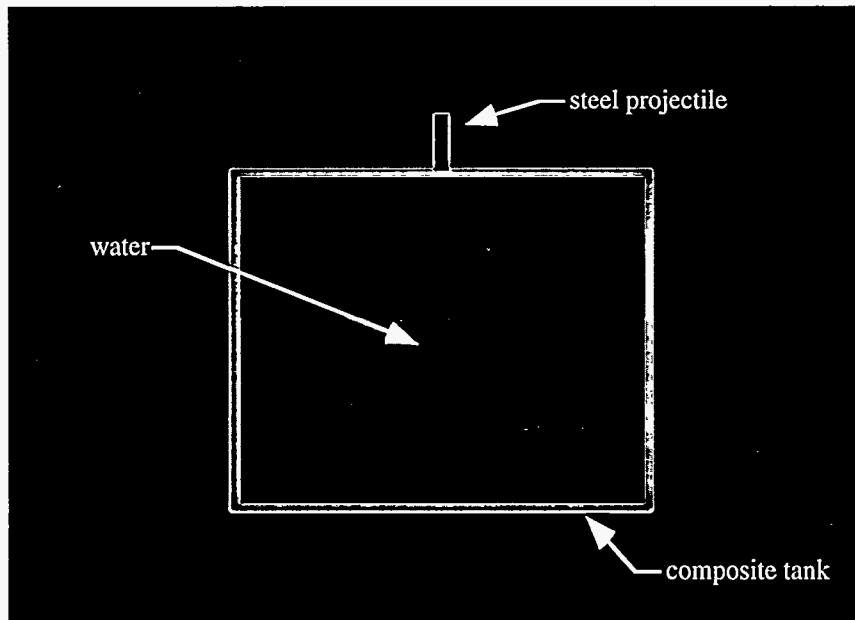


Figure 4: Two-dimensional, axisymmetric hydrodynamic ram simulation involving the impact and penetration of a 23-mm steel projectile into a graphite/epoxy composite fuel tank. The configuration shown is the reference configuration at the time of projectile impact.

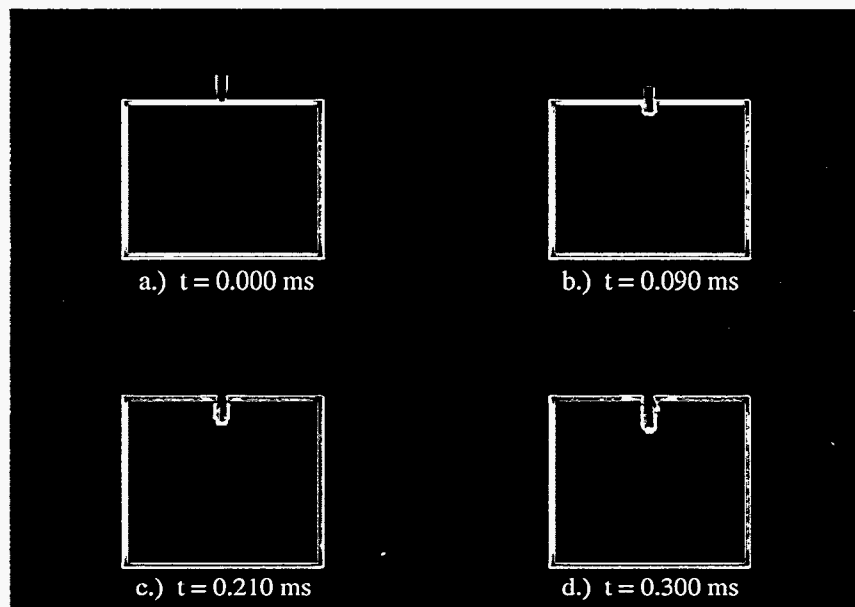


Figure 5: The fuel tank in deformed configurations at 0.09, 0.21, and 0.30 ms after initial projectile impact. Note that the behavior of the solid fuel tank, the solid projectile, and the liquid fuel are fully coupled.

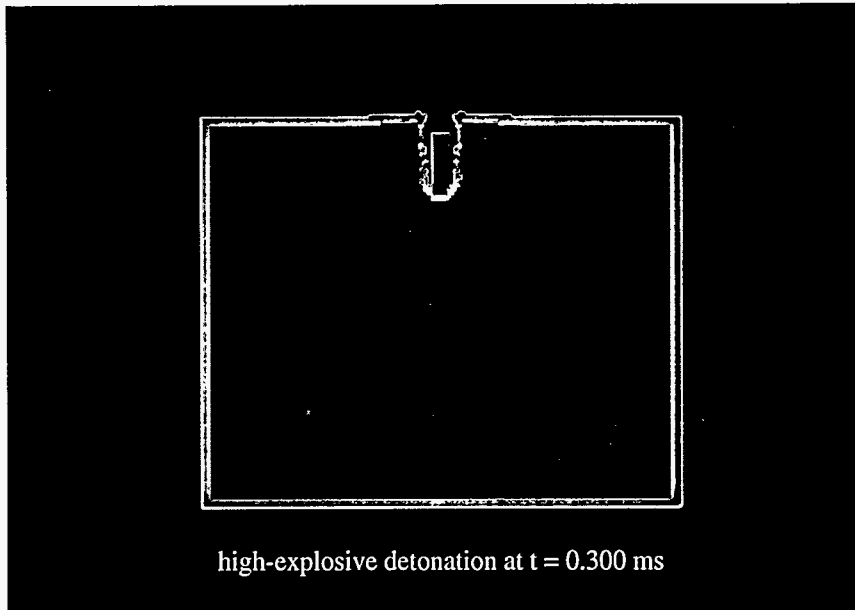


Figure 6: An enlarged view of the deformed fuel tank at $t = 0.30$ ms. Note that the projectile has completely perforated the composite plate and that the plate is deforming upward due to the nearly incompressible nature of the contained fluid.

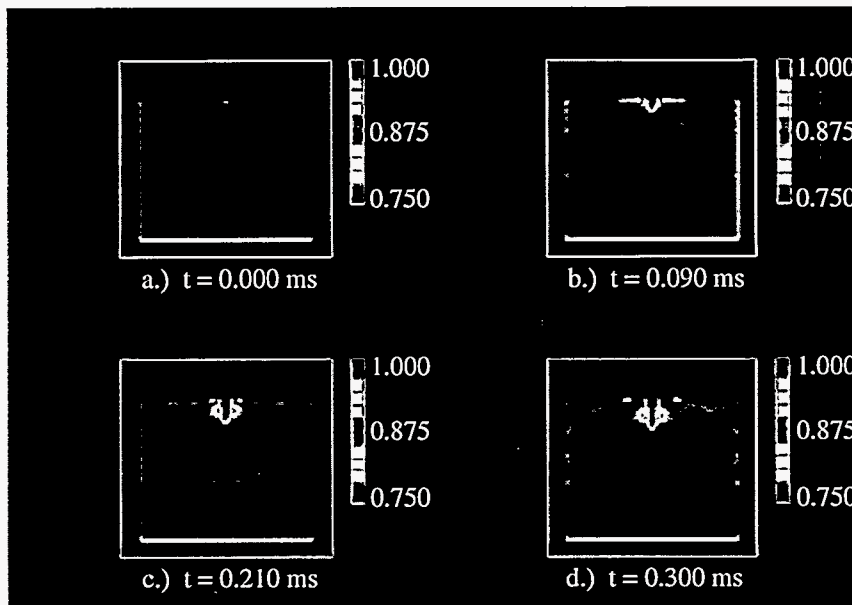


Figure 7: Water density at 0.09, 0.21, and 0.30 ms after initial projectile impact. Notice the propagation of a weak shock front originating from the initial impact event and the cavitation zones in the water on either side of the projectile path.

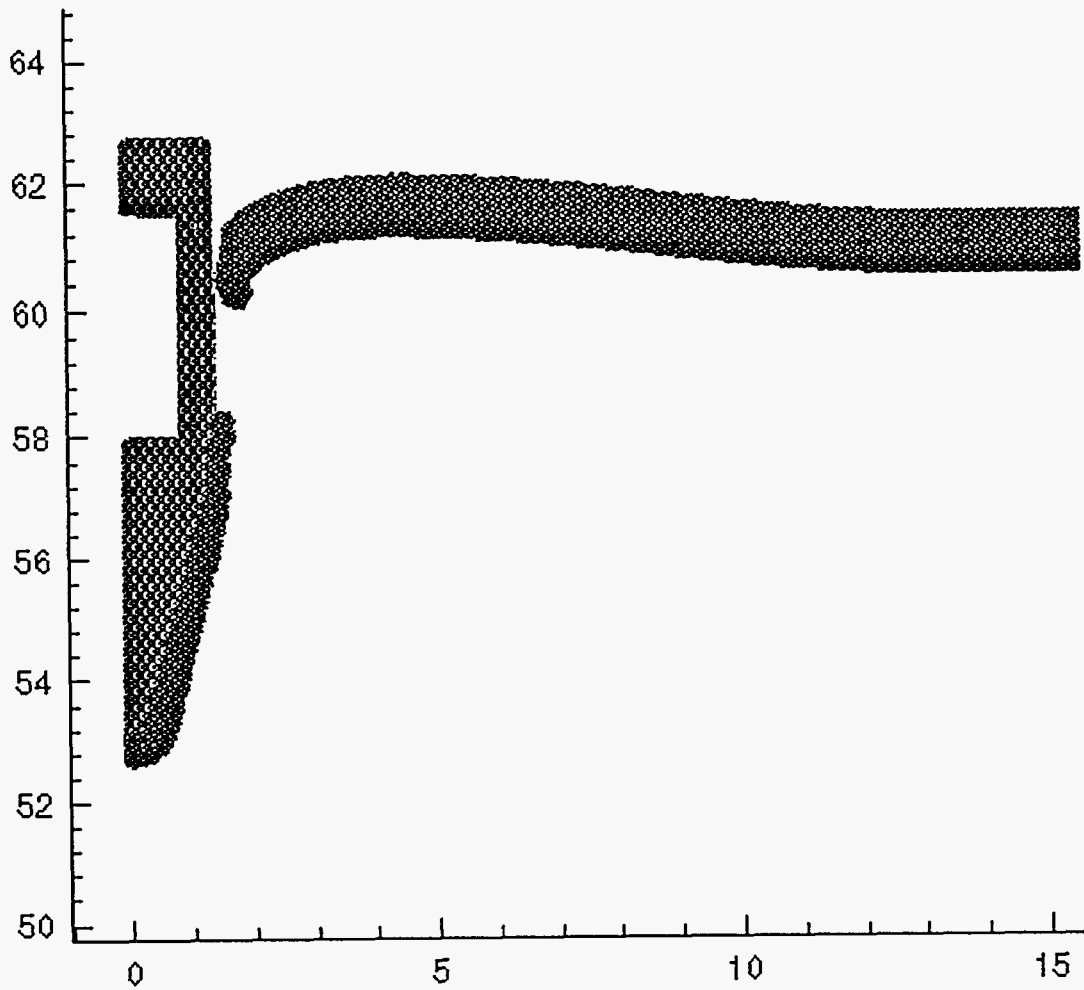


Figure 8: Deformation of the high-explosive projectile and the fuel tank entrance plate at 220 ms after initial projectile impact. Notice that the entrance plate has completely failed due to the strain-to-failure model that was incorporated into the calculation.

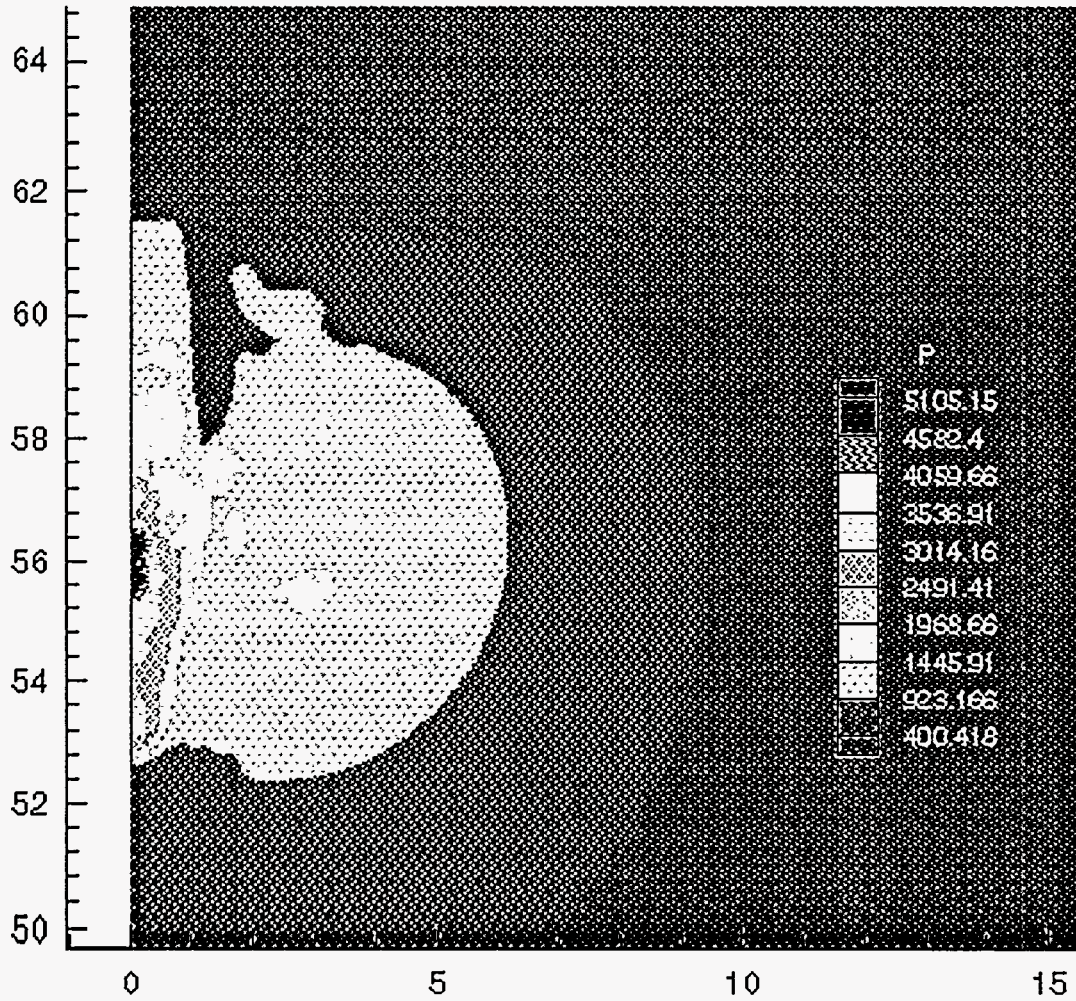
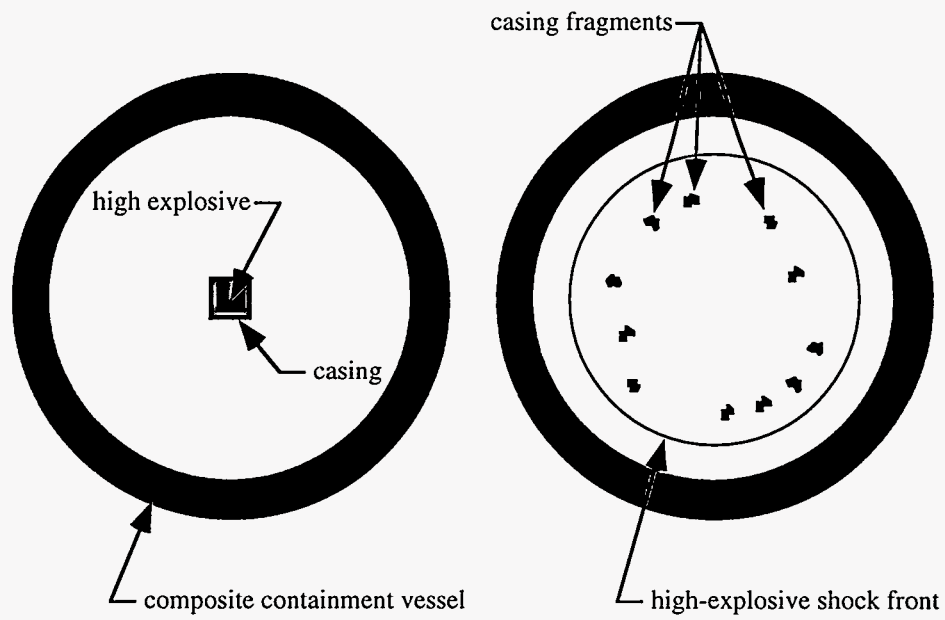
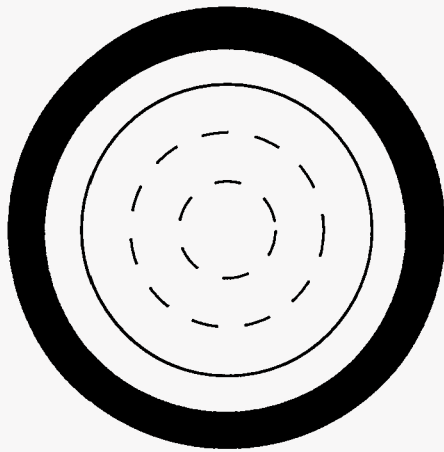


Figure 9: Fluid pressures at 220 ms after initial projectile impact. Evidence of the Eulerian diffusion of explosive products can be seen in this plot. The resulting pressure wave is much stronger than the pressure wave that results from the initial impact event alone.



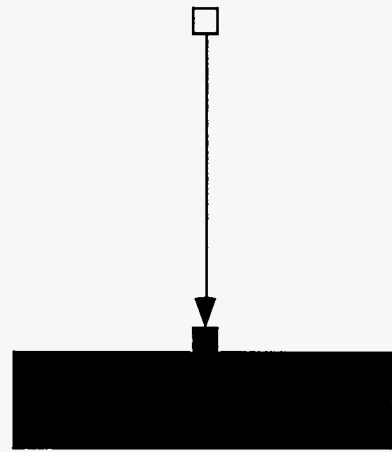
(a)

(b)



problem 1: shock-wave loading of a composite containment vessel

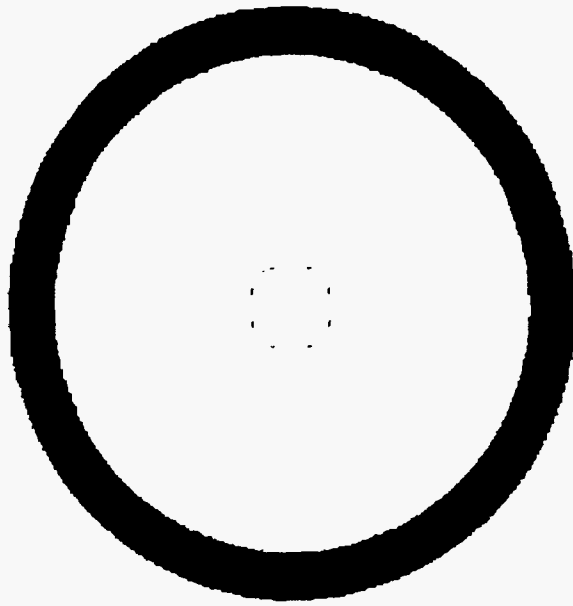
(c)



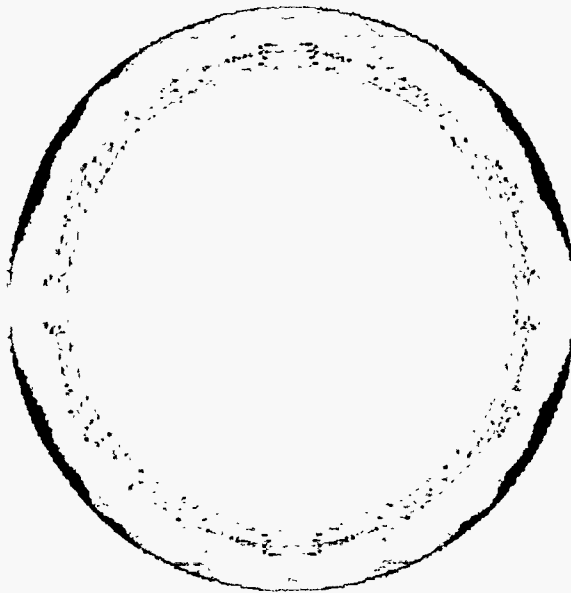
problem 2: fragment impact and penetration of a composite plate

(d)

Figure 10: High-explosive detonation within a spherical composite containment vessel. The problem is decoupled into two separate problems involving shock wave propagation and fragment impact and penetration.



(a) shock wave propagation



(a) pressure wave loading of the composite vessel

Figure 11: Shock-wave loading of a composite containment vessel. Despite the high pressures involved, the deformations of the vessel walls remain small, and the levels of stress do not approach critical failure values.



(a) $t = 0.025$ ms



(b) $t = 0.060$ ms



(c) $t = 0.100$ ms

Figure 12: High-explosive casing fragment impact and penetration of a thin composite plate. Notice the shock wave propagation through the solid material and the free-surface creation in the impact crater.